ADVANCING EARTH AND SPACE SCIENCES

JGR Earth Surface

RESEARCH ARTICLE

10.1029/2024JF008051

Automated Mapping of Braided Palaeochannels From Optical Images With Deep Learning Methods

F. Vanzani[1], **P. Carbonneau**[2], **and A. Fontana**[1]

[1]Department of Geosciences, Università Degli Studi di Padova, Padova, Italy, [2]Department of Geography, University of Durham, Durham, UK

Key Points:

- An Attention-UNet model was trained to segment fluvioglacial braided palaeochannels from aerial orthophotos over an area of 242 km^2
- The model was tested in four other sites characterized by similar traces in Italy and Montenegro showing a good generalization capability
- As one of the first applications of deep learning to palaeohydrology we show the potential to map complex traces on alluvial surfaces

Supporting Information:

Supporting Information may be found in the online version of this article.

Correspondence to:

F. Vanzani,
federica.vanzani@phd.unipd.it

Citation:

Vanzani, F., Carbonneau, P., & Fontana, A. (2025). Automated mapping of braided palaeochannels from optical images with deep learning methods. *Journal of Geophysical Research: Earth Surface*, *130*, e2024JF008051. https://doi.org/10.1029/2024JF008051

Received 20 SEP 2024
Accepted 24 JAN 2025

Author Contributions:

Conceptualization: F. Vanzani, A. Fontana
Funding acquisition: A. Fontana
Methodology: F. Vanzani, P. Carbonneau
Software: F. Vanzani, P. Carbonneau
Supervision: P. Carbonneau, A. Fontana
Writing – original draft: F. Vanzani
Writing – review & editing: F. Vanzani, P. Carbonneau, A. Fontana

Abstract

The increasing availability of remotely sensed data has provided an enormous quantity of information for studying the geomorphology of exposed surfaces of alluvial plains. In many cases, the key for reconstructing their formation lies in the recognition of optical traces related to abandoned palaeochannels and their morphometric characteristics. Abundant braided palaeohydrographic traces are documented in alluvial plains of northern Italy, where large sectors of the present surface correspond to landforms related to fluvioglacial systems supplied by Alpine glaciers during the Last Glacial Maximum (LGM). Nevertheless, the complexity of multichannel patterns, the overlapping field division systems and urbanization, hinder the efforts to manually map these traces. In this work, we used high-resolution aerial photos of the proximal sector of the Friulian Plain (NE Italy) to train an Attention-UNet deep learning algorithm to segment palaeohydrographic traces. The trained model was used to automatically recognize braided palaeochannels over 232 km^2. The resulting map represents a significant step for investigating the long-term alluvial dynamics. Moreover, we assessed the robustness of our method by deploying the model in three other areas in northern Italy with comparable characteristics, as well as in Montenegro, near Podgorica. In each case, the braided pattern was successfully mapped by the algorithm. This work highlights the breakthrough potential of deep learning methods to rapidly detect complex geomorphological traces in cultivated plains, taking into consideration advantages, challenges and limitations.

Plain Language Summary

Revealing how the landscape of partly urbanized alluvial plains has changed in the last ten thousand years can be achieved through the identification of traces of ancient river channels which are visible in satellite images and aerial photos. For example, a great quantity of these traces is present in the plains in northern Italy, where the surface is largely made of braided ancient channels related to the Last Glacial Maximum (28,000–19,000 years BP). However, manually mapping these channels is very challenging due to the complexity of the braided pattern, the overlapping of dense field divisions and the presence of urban centers. In this work, we trained an Artificial Intelligence to automatically map the relict river channels over a sector of the alluvial plain of over 200 km^2. The model also successfully mapped braided ancient channels in four other sites in northern Italy and Montenegro, suggesting that this model could be used in more alluvial plains in Italy and Europe. The positive results are one of the first implementations of artificial intelligence in the field of landscape evolution over long time intervals and will allow scientists to obtain detailed maps of complex geomorphological ancient features.

1. Introduction

In the past 10 years, the rapid rise of deep learning algorithms such as Convolutional Neural Networks (CNNs) has dramatically changed remote sensing studies. Commonly deployed for object recognition (LeCun et al., 2015), and medical science images (Litjens et al., 2017), deep learning algorithms have also been subsequentially adapted to land cover classification (Kussul et al., 2017), urban scenes segmentation (Cordts et al., 2016), crop studies (Jha et al., 2019), sedimentary geology (Zhang, S. et al., 2020), landslides detection and monitoring (Huang et al., 2020), and many more applications (e.g., Camps-Valls et al., 2021; Ma et al., 2019). CNNs have yielded unprecedented results in river science (Carbonneau & Bizzi, 2024; Kabir et al., 2020) enabling classification, mapping, and quantification of fluvial landforms (e.g., Carbonneau, Belletti, et al., 2020; Carbonneau, Dugdale, et al., 2020).

CNNs are a type of deep learning supervised model which works by performing convolutions on the image and backpropagating the loss with respect to the training data in order to optimize weights held in the convolution

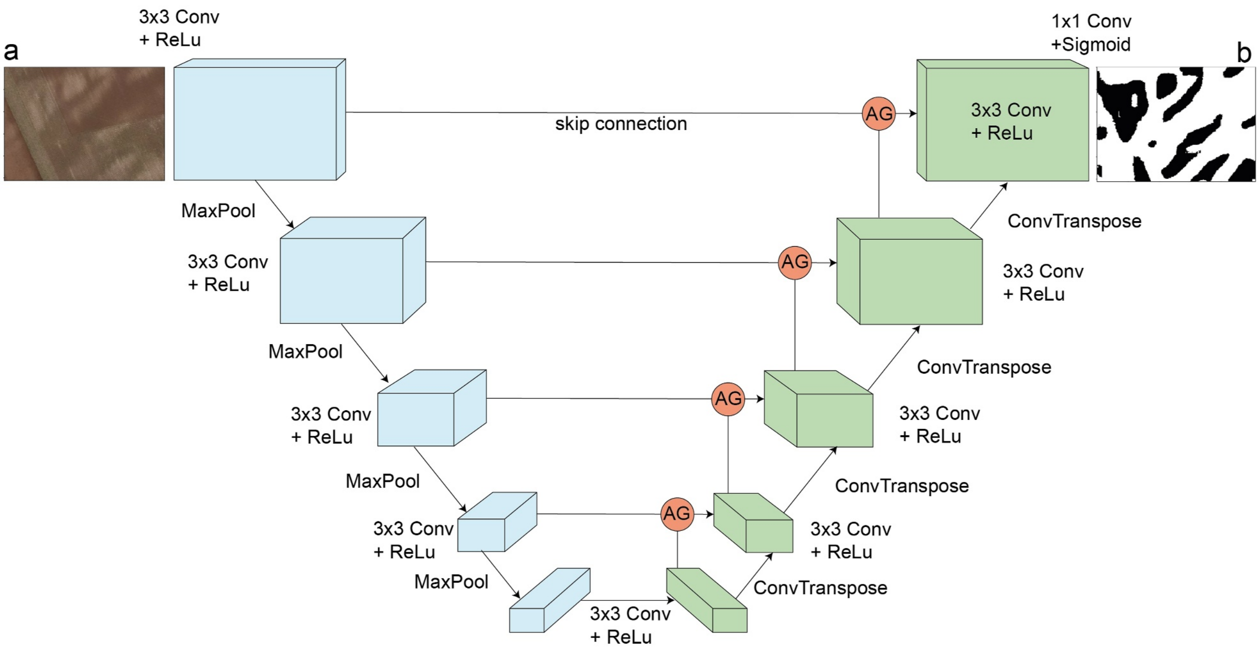

Figure 1. Simplified architecture of the Attention-UNet used in this work. (a) Input RGB image tile with size of 256 × 256 m; (b) output binary segmented tile with size of 256 × 256 m. In blue, the encoder part and in green, the decoder part of the algorithm. Skip connection indicates which feature maps from the encoder and decoder are taken as input of AG and then concatenate before deconvolution (ConvTranspose). AG represents the attention gates.

kernels (Camps-Valls et al., 2021). In remote sensing applications, one of the common tasks of CNNs is to segment and identify selected features and classes of objects (Ma et al., 2019). Semantic segmentation refers to the task of assigning each pixel of the input image to a class (Chen et al., 2018; Tuia et al., 2021). Models implemented in the field of remote sensing are usually made of an encoder–decoder structure (Long et al., 2014) such as UNets (Ronneberger et al., 2015). This architecture consists of a series of convolutional layers extracting feature maps with increasing depth and decreasing spatial extent (the encoder), followed by a symmetrical part of deconvolutional layers that up-samples feature maps to a tensor with the same size as the input tensor. The encoder permits feature maps in deeper layers to receive spatial information from increasingly large areas, whilst the decoder is connected to the corresponding feature maps in the encoder through skip connection, which consists of stacking them before the deconvolutional layer. In this work, we trained a type of UNet referred to as Attention-UNet (Oktay et al., 2018), which introduces attention gates (AG) to skip connection in the decoder. AG takes feature maps from the decoder and the corresponding feature maps from the encoder as inputs, which are summed element-wise so that aligned weights will become larger, the result is then passed through an activation layer collapsing its dimension and a sigmoid layer rescaling the vector between 0 and 1. The weights are then multiplied to the feature map coming from the encoder before it is stacked to the corresponding map in the decoder and passed through the deconvolutional layer (Oktay et al., 2018). This process leads to larger weights being multiplied to relevant parts of the image, so that during training the model will be encouraged to focus on these areas (Figure 1). Attention-UNets were originally proposed for the segmentation of medical images, but have been successfully implemented in geosciences from landslide detection (e.g., Nava et al., 2022) to palaeochannel identification in seismic images (e.g., Zhong et al., 2024).

In most of the large alluvial plains and alluvial fans, the key for reconstructing the past landscape evolution lies in the recognition of abandoned channel belts (e.g., In Berendsen & Stouthamer, 2001; Kiss et al., 2014; Oya, 1995) are often visible through high resolution remotely sensed data (e.g., Waller et al., 2018). Currently, the surface of alluvial plains is often affected by anthropogenic activities that strongly reworked or sealed the original topography, due to plowing and leveling operations related to agriculture, as well as urban expansion. These disturbances have been going on for millennia in most parts of the continents or more recently in other regions (e.g., In Brown, 1997; In Gibling, 2021; Prümers et al., 2022). In general, besides eroding the original landforms of the alluvial plains, the historical and modern agricultural practices led to exposure of the traces of palaeohydrographic features, that in many environments would be otherwise covered by forest and practically invisible through remote sensing.

This work focuses on the identification of gravelly braided palaeohydrography, a river morphology characterized by multiple intersecting channels separated by exposed fluvial bars. In all the cases identified in this study, the petrographic composition of the gravels is strongly dominated by carbonate rocks. These palaeohydrographic systems cover a large sector of the alluvial plains, and are characterized by alternating abandoned channels and fluvial bar deposits that mainly form as fluvioglacial outwashes in colder climates and have at least about 20 ka. Thus, the surface has been exposed to atmospheric and biological processes for at least 20 ka. This has led to the formation of well-developed soils, characterized by the accumulation of new-formation clays with a typical reddish color due to the abundance of residual oxides. The soil profile overlays the original topography of alternating fluvial bars and channels, and ancient and modern plow activities have removed part of it, exposing the top portion of the carbonate gravelly bars, whilst ticker reddish argillic horizons have been preserved in correspondence of the channels, which are slightly depressed and allowed a thicker soil formation and accumulation (Figure 3). As a consequence, the modest difference in topography between channels and bars is accompanied by a clear contrast in the spectral signature revealed by RGB imagery. In particular, the signature of the clay overlaying the channel is darker, whilst the carbonate gravels exposed over the fluvial bars are lighter. In this work, we took advantage of this stark chromatic and tone difference to distinguish the multiple intersecting channels of the braided palaeohydrographic system. Hence, for the aim of this study, the words palaeochannel and palaeohydrographic trace refer to the darker clays overlaying the abandoned channels, whilst the lighter spectral signature of the exposed bars is considered as the background.

Mapping these palaeohydrographic tracks is generally of paramount importance for supporting territorial planning and land management, because of the specific geotechnical, hydrogeological and environmental properties (e.g., lithology, permeability and depositional geometries) connected to the different portions forming the alluvial landforms and related deposits (e.g., In Bridge, 2003; Oya, 1995).

It is worth noting that the large majority of the geomorphological mapping through remotely sensed images considers only the distal portion of the plains, where the relict hydrographic traces are single-channel features and they display a sinuous or meandering planform (e.g., Cassiani et al., 2020; Mahammad & Islam, 2021). A very restricted number of studies carried out detailed investigations on sectors with braided palaeochannels and several of them considered rather limited zones, mainly in the recent proglacial sandar of southern Iceland (e.g., Waller et al., 2018). On the contrary, a lot of attention has been devoted to active braided and wandering rivers, because of the feedback in understanding the fluvial processes, the possibility to check in the field the simulations obtained by numerical models and to perform automatic or semi-automatic recognition of fluvial landforms (e.g., Carbonneau & Bizzi, 2024; Ziliani & Surian, 2012).

Despite their visibility in remotely sensed data, manually mapping relict braided traces is generally very challenging. Their widespread distribution, the overlapping shapes, together with the presence of intersecting roads, urban centers and different croplands, make manual mapping a time-consuming and often frustrating effort for researchers. Consequently, geomorphologists may abandon the idea of mapping these traces altogether or limit this activity to small areas.

Our work aims to pioneer the implementation of an Attention-UNet architecture for the fast mapping of palaeohydrographic traces in alluvial plains, with special focus on braided patterns. This study also seeks to address challenges such as: the inconsistent appearance of traces due to diverse croplands, intersecting roads, and urbanization; and the limited availability of data sets. Here, we present and discuss the results, highlighting the level of accuracy, limitations and advantages of applying these kinds of automated mapping workflows. As one of the first implementations in the field, we also aim to encourage scientists working on late Quaternary landscape evolution to improve the use of similar deep learning algorithms in their research.

As a test site, we selected a portion of NE Italy, which corresponds to one of the alluvial plains where the relict traces are particularly evident at the surface. In fact, their detailed mapping allowed significant advances in deciphering both the evolution of the fluvial systems and the archaeological patterns (e.g., Cassiani et al., 2020; Fontana, Monegato, et al., 2014; Ninfo et al., 2009; Tozzi & Harari, 1984). Nevertheless, investigations carried out in this area mostly neglected the proximal sector of the plain where, even if braided pattern is dominant, it has been mainly mapped with a general symbology indicating the occurrence of ancient multiple palaeochannels, but

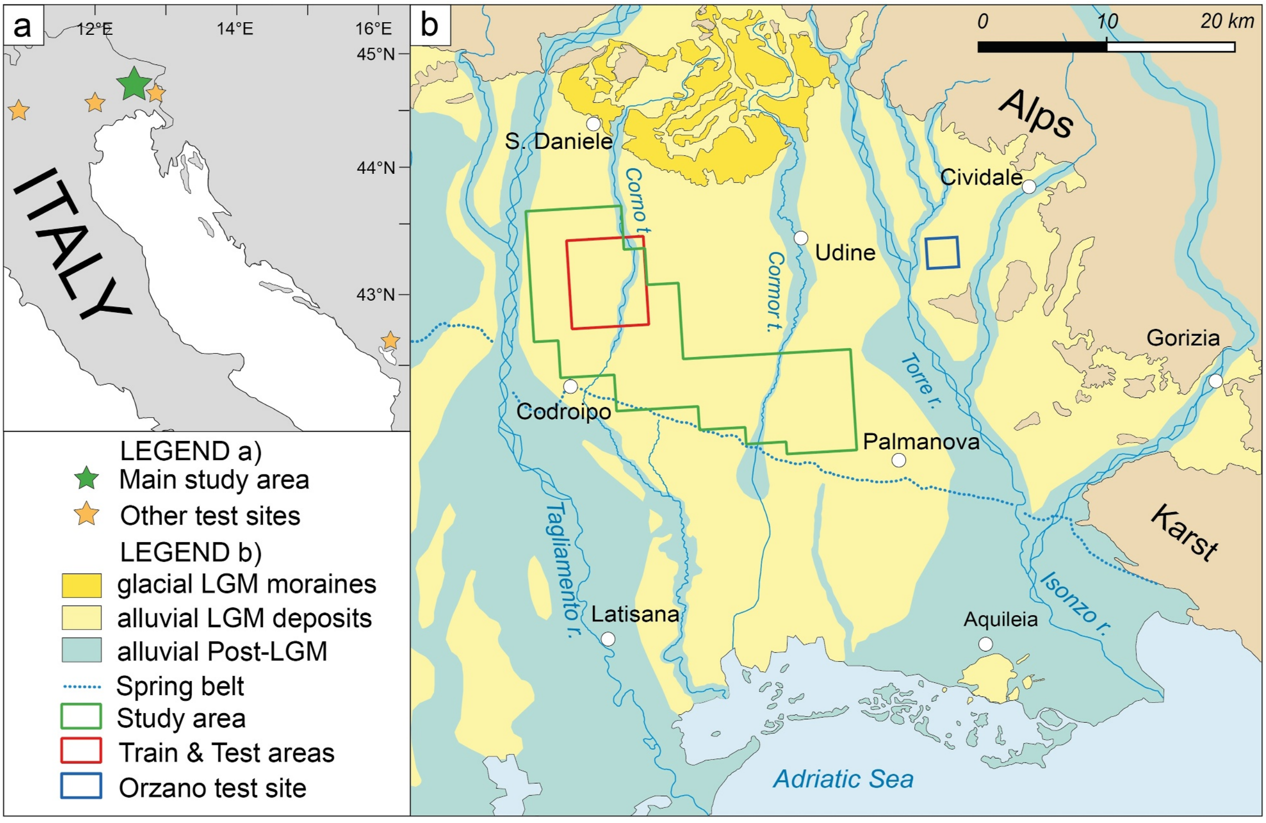

Figure 2. (a) Locations of the main study area (green star) and other selected test sites (yellow stars); (b) Detailed map of the train and test areas with indication of geological units forming the surface of the Friulian Plain.

avoiding the details of the relict landforms (Bondesan et al., 2015; Fontana et al., 2019). At the same time, the area is currently characterized by rather large active streams that are fed by the Alps (i.e., Isonzo, Torre, Tagliamento, Piave and Brenta rivers) and display a typical braided pattern in the apical sector of the alluvial plain (Surian & Rinaldi, 2003; Tockner et al., 2003).

2. Setting

The main study area is located in the Friulian Plain in north-eastern Italy and corresponds to part of the apical sector of the alluvial megafans of the Tagliamento, Corno, Cormor and Torre streams (Figure 2). These depositional systems were formed during the Last Glacial Maximum (LGM, 28–19 ka BP), when they were directly fed by the huge liquid and solid discharge supported by the front of the glacier occupying the mountain catchment of the Tagliamento River (Fontana et al., 2008, 2014b), which in that period reached the plain and formed the morainic amphitheater (Monegato et al., 2007). Since about 19 ka cal BP, almost all the proximal sector of the Friulian Plain was already abandoned by the alluvial activity and Corno and Cormor transformed from major glacial outwashes to minor streams with local hilly catchments. The passage from fluvioglacial to fluvial conditions led the Tagliamento and Torre rivers to strongly reduce their solid and water discharge; thus, during the Late Glacial and Holocene, they were active only in the distal portion of their megafan (Fontana et al., 2008).

The study area is made of gravelly fluvioglacial sediments associated with braided channel belts, that deposited during the second part of the LGM (i.e., 24–19 ka cal BP) and that extended downstream up to the present spring line , while downstream of this boundary, the LGM deposits are dominated by silt and clay (Fontana, Monegato, et al., 2014, Fontana et al., 2008). The area where the model has been trained has an extent of 42 km^2 (Figure 2) and, as well as the other test sites, is characterized by an abundance of braided palaeohydrographic traces visible through optical remotely sensed data (aerial photos and satellite images). The visibility of these marks is mainly the result of pedogenetic and anthropogenic activities.

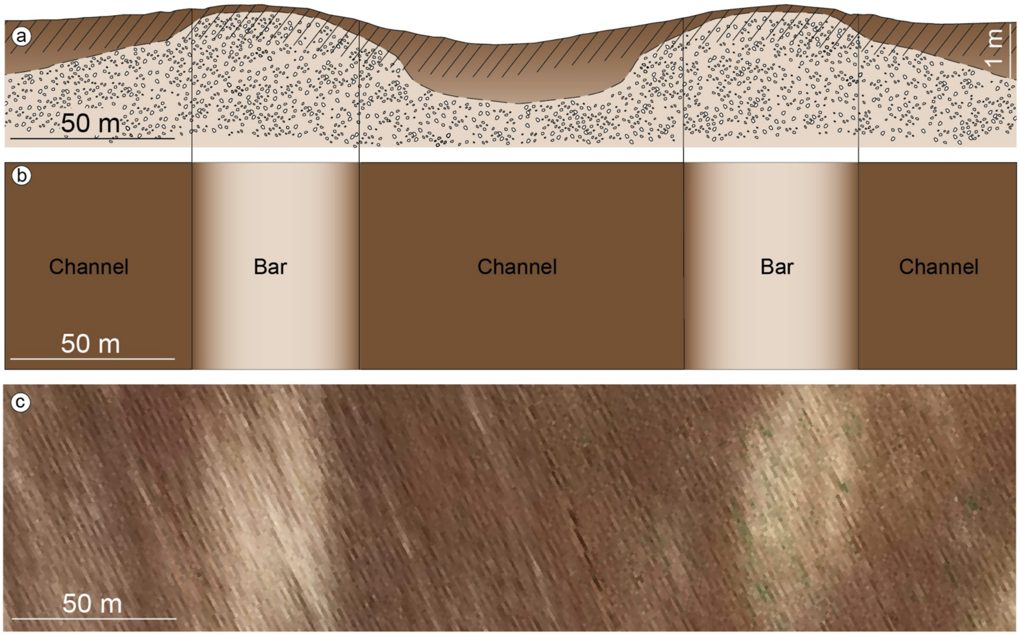

Figure 3. The appearance of palaeohydrographic traces in the study area. (a) Schematic cross-section of the study area surface corresponding to the schematic planar view, with vertical exaggeration 16x. The inclined lines are plowing furrows and highlight the strong reworking of the topsoil; (b) Schematic planar view of the top surface corresponding to the aerial photo example. Lighter colors indicate a fluvial bar, darker colors a channel; (c) Example of aerial photo from the training data set corresponding to the schematic representation above.

The petrographic composition of the gravels fed by the Tagliamento glacier is strongly dominated by carbonate rocks (around 70%), such as limestone and dolostone, and the prolonged geomorphological stability of the investigated area has been exposing the top portion of these sediments to atmospheric and biological processes for the last 20 ka (Zanferrari, Avigliano, Grandesso, et al., 2008, Zanferrari, Avigliano, Monegato, et al., 2008). Another significant property of the study area is the limited presence of urbanized zones, with small scattered villages, but the large majority of the topographic surface corresponds to cultivated cropland.

The sedimentologic and pedologic characteristics described for the main study area are also quite similar in the other smaller areas that have been selected with the aim of testing the methodology and assessing the generalization capability of the automated mapping model. They are also characterized by braided paleochannels and dominated by carbonatic clasts that display a high visibility in RGB aerial images. The sites are located at an increasing distance from the area where the model was trained and they were formed by different fluvial and fluvioglacial systems from the one fed by the Tagliamento glacier. They are the areas of Orzano (Friulian Plain), Montebelluna (Venetian Plain), Montichiari (Lombard Plain), and the zone near the airport of Podgorica in Montenegro (alluvial fan of Cem River) (Figure 2).

The area of Orzano (46°3'13.50'N, 13°21'55.81"E) extends for 12 km^2 and is located in the eastern portion of the Friulian Plain, only 9 km east from the main study site. The surface was formed by gravelly braided channels of the Natisone River, which during LGM was fed by the glacier occupying the mountain catchment of the Isonzo River (Fontana, 2024).

The zone of Montebelluna (45°43'38.52"N, 12°1'20.02"E) has an area of 3 km^2, is located in the Venetian Plain, about 80 km west of the main study area, and it is part of the apical sector of the alluvial megafan of Montebelluna. This was formed by the Piave River in a pre-LGM period and likely at the end of the Middle Pleistocene, during the penultimate glaciation (Fontana, Mozzi, & Marchetti, 2014). The top surface displays traces of braided channels formed by fluvial or fluvioglacial gravel deposits.

The Montichiari site (45°26'50.73"N, 10°20'22.20"E) has an extent of 15 km^2 and is located in the Lombard Plain, 210 km west of the main study area. The surface is made of gravelly braided channels that belong to the apical sector of the LGM alluvial megafan of the Chiese River (Fontana, Mozzi, & Marchetti, 2014).

The last site of comparison is in Montenegro (42°22'57.88"N, 19°17'36.17"E) extending for 6 km^2 and is located near the airport of Podgorica, about 600 km south–east of the main study area. The analyzed surface is part of the gravelly alluvial fan of the Cem River, that has a mountain catchment in the Dinaric Alps between Montenegro and Albania and which was interested by glacial advances during the last Pleistocene glaciations (Hughes et al., 2011; Radusinović & Pajović, 2024).

It is worth noting that the main study area is bounded on the west by the present channel of the Tagliamento River, which is the reference stream for investigating the semi-natural dynamic of gravelly braided rivers in the Alps (e.g., Bertoldi et al., 2009). Thus, the reconstruction of the morphometry of a large portion of the braided alluvial plain formed by this river system in the past could support an important comparison for understanding the present processes. 3 Methods and Workflow.

The original data set for the main study area consists of aerial orthophotos acquired in May and June of 2012 by the Civil Protection of the Regione Autonoma Friuli Venezia Giulia, which can be freely viewed on the Geoportal of the Regione Autonoma Friuli Venezia Giulia (https://eaglefvg.regione.fvg.it). They were collected using an Ultracam Eagle camera—manufactured by Vexcel Imaging GmbH—mounted on a Pilatus Porter PC-6 airplane. They have a spatial resolution of 0.10 m in RGB color bands.

In this work, we obtained the data set of the entire Friulian Plain, from which we selected the study area boundaries. Afterward, we down sampled the orthophoto to 1 m/px resolution to improve the performance of the following steps.

We pre-processed the images by selecting a training area of 6 × 7 km from the original study area, consisting of 607 tiles obtained by dividing the original photos in 256 × 256 m tiles. QGIS software (version 3.22.5) was used to manually draw and label the palaeochannels over this area. For the scope of this work, palaeochannel boundaries were defined as the edges of the dark argillic soils visible in the photos. Moreover, to limit user bias, the entire manual labeling process was performed by the same user. Since a major issue in mapping palaeohydrographic traces in the study area is the presence of modern road patterns overlaying the geomorphological evidence, we intervene on the ground truth labels by specifically drawing palaeochannels considering their continuity, ignoring interrupting infrastructures, and labeling the tracts of crossing roads as part of the palaeohydrography. Conversely, if large urban centers or vegetated fields were present, no ground truth labels were drawn. Labels were subsequentially converted into binary rasters.

The orthophoto and the labels were divided into tiles of 256 × 256 m. Dimensions and spatial resolution of the tiles were chosen as a compromise between the size of the palaeochannel traces–which we observed to vary greatly from a few meters to over 100 m in width–and the time required to train a deep learning model. This compromise aimed to ensure that the dimensions of the palaeochannels fit inside the tile size. The entire workflow of this study is shown in Figure 4. Images and corresponding label tiles were randomly subdivided into training and test data sets, with the test data set consisting of 111 tiles. Afterward, due to the small number of tiles, data augmentation was used on the training data set to significantly increase its size. Augmentation consists of various techniques ranging from pixel to spatial transformations, which create new training samples from the existing images (Shorten & Khoshgoftaar, 2019). The implementation was carried out through the Albumentation (version 1.3.1) library on Python (Buslaev et al., 2020). The final augmented data set was obtained using a combination of the following techniques: crop, vertical and horizontal flip, transpose, 90° rotation. Specifically, RandomCropSize clips a random part of the image–limiting the height and width of the crop to 120 × 120 px—and resizes it to the original 256 × 256 px;vertical and horizontal flip switch the input vertically and horizontally, respectively;transpose inverts rows and columns; RandomRotate90 randomly rotates an image of 90° one or more times. The final data set consisted of 24,800 tiles. To tackle class imbalance between features and background, tiles with no palaeochannel present were excluded, reducing the total number of tiles to 21,874. Finally, this data set was randomly divided into training and validation data sets, with the validation set corresponding to 20% of the 21,874 tiles.

To process the images, we implemented a CNN model through the Keras (version 2.10.0) and Tensorflow (version 2.10.1) libraries in a Python environment (version 3.10). Various model architectures were tested, from FCN with ResNet (He et al., 2016) and ConvNext (Liu et al., 2022) as encoding backbones, to simple UNets (Ronneberger et al., 2015). At the end, the Attention-UNet (Oktay et al., 2018) architecture was chosen.

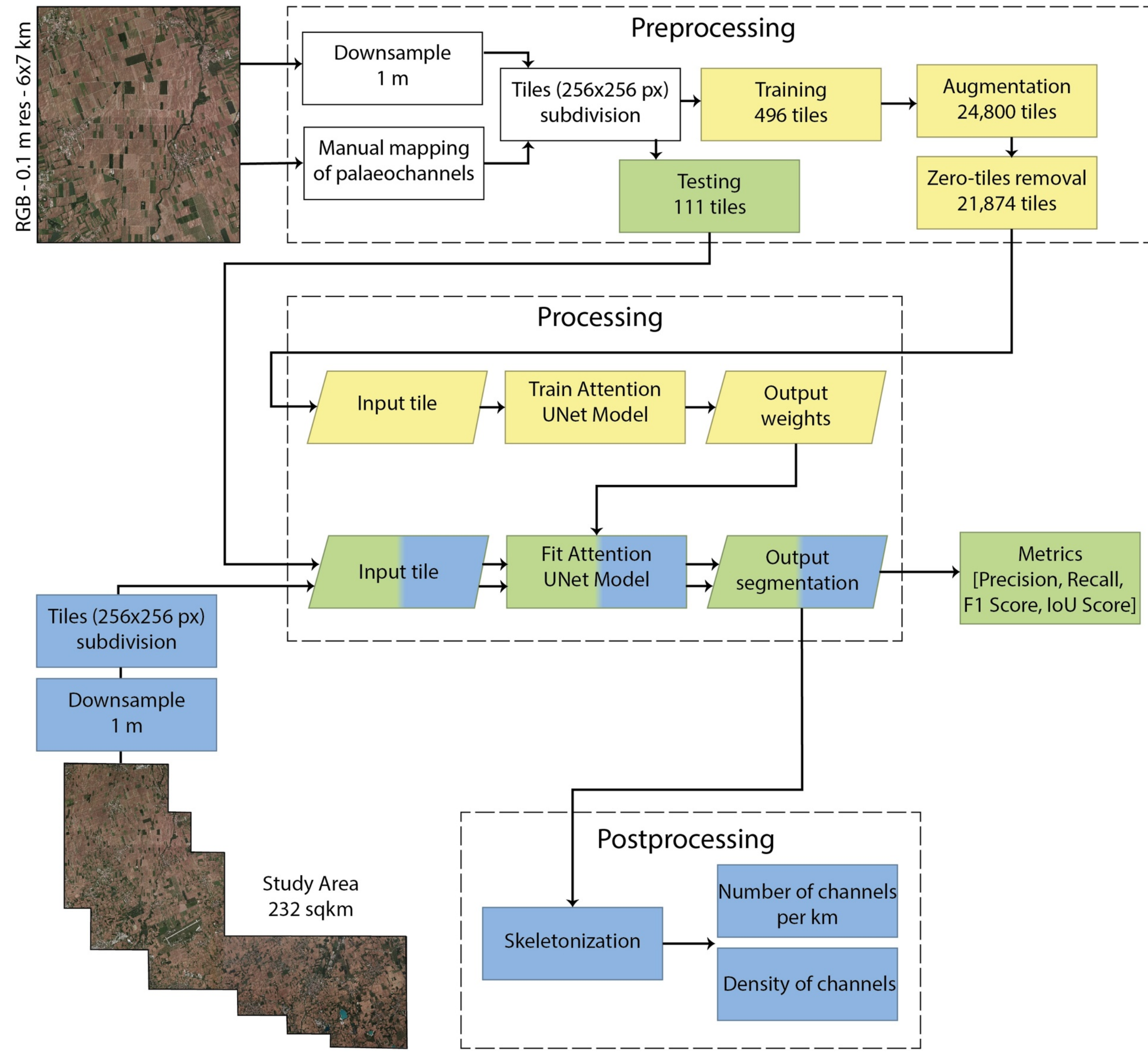

Figure 4. The workflow diagram, highlighting the main steps in the application of the deep learning algorithm. Different colors are used to distinguish processes applied to the training set (yellow), test set (green), and the entire study area (blue).

The choice of using an Attention-UNet model in this work was based on two main considerations. Firstly, we investigated other types of segmentation models, such as FCNs with ResNet50 or ConvNextTiny as backbones in the encoder part of the algorithm, but found that the high number of trainable parameters–30 million and 29 million, respectively–coupled with the small size of our data set, led to severe overfitting issues. In contrast, the smaller size of UNets seemed to perform much better and avoid overfitting on the validation data set. Secondly, Attention-UNets have been successfully adopted in geomorphology in recent years (Nava et al., 2022; Zhong et al., 2024), specifically to deal with binary segmentation problems and high-class imbalance data sets. In general, we observed that when attention blocks were added to a simple UNet architecture, the model was greatly encouraged to focus on the segmentation of palaeochannels, and the performance on the test data set was vastly improved. In the study area of the Friulian Plain, the attention gates work exceptionally well in training the UNet to not give much importance to the complex background of forested, urban, and crop areas; rather the model learned to focus on identifying the braided pattern of palaeochannels. This advantage, coupled with the small number of trainable parameters characterizing the Attention-UNet model, allowed us to train a successful deep learning algorithm.

Attention gates were implemented following the methodology described by Abraham and Khan (2018) and Nava et al. (2022). The model architecture is made up of four encoding blocks and four decoder blocks. Each encoding block consists of two convolutional layers (convolution + batch normalization + activation) followed by a maxpooling. The number of filters in the first encoding block is 8 and 128 in the last one (Figure 1). This choice is mainly based on the computational limits of training a model with a large number of filters. Each decoder block is made by an attention gate block applying weights to the feature map coming from the encoder, followed by a deconvolutional layer applied to the feature map in the decoder, and a concatenation of the two resulting maps. In the decoder, we used the He Uniform distribution (He et al., 2015) to initialize weights. In order to tackle the overfitting issue, we added Dropout equal to 0.1 at the end of each encoder block. Dropout is a common technique used in CNNs which consists in dropping random nodes during training to improve the generalization of the model, especially useful for small data sets such as the one used in this work (cf. Srivastava et al., 2014). Similarly, a kernel regularizer in the form of weight decay ($L2 = 0.01$) was used in each convolutional layer in the encoder blocks (Cortes et al., 2012). The addition of these two techniques aimed to improve the overfitting risk caused by the small input data set. The loss function optimizer is Adam (Kingma & Ba, 2014) and the loss function Dice Loss (Milletari et al., 2016), following the implementation of Abraham and Khan (2018) and Nava et al. (2022).

$$\text{Dice Loss} = 1 - \frac{2\sum_{i=1}^{N} p_i g_i}{\sum_{i=1}^{N} p_i + \sum_{i=1}^{N} g_i} \tag{1}$$

Equation 1 represents the dice loss of a binary segmentation. p_i is the predicted pixel value and g_i is the ground truth value. N is the total number of pixels. The dice loss is a measure of the overlap between a predicted segmentation mask and the ground truth mask. It is defined as the intersection of the two masks divided by their sum.

The number of trainable parameters in the model was 571,556. The batch size we used was 32 as a compromise between computational costs and better performance. The learning rate was 5e−5. The entire architecture and implementation is described in detail at https://doi.org/10.5281/zenodo.13762915.

After training, we derived the following metrics: Precision, Recall, F1-Score, and IoU-Score. Precision is defined as the ratio between the number of true positives–pixels correctly classified by the model–and the sum of true positives and false positives. If the number of false positives is equal to zero, then precision is equal to one. Precision measures the ability of the model to not classify background pixels as features (Equation 2). On the contrary, recall is the ratio between true positives and the sum of true positives and false negatives. If the number of false negatives is equal to zero, then recall equal to one. Recall measures the capability of the model to identify all pixels belonging to the feature class (Equation 3). F1-Score is the harmonic mean between precision and recall, and it measures the performance of the model based on class, essentially permitting to focus on maximizing both precision and recall (Equation 4). IoU-Score–which stands for Intersection over Union score–is another evaluation metric, specifically designed for segmentation models. It is defined as the ratio between true positives and the sum of true positives, false positives, and false negatives. It measures the overlap between prediction and ground truth (Equation 5).

$$\text{Precision} = \frac{\text{TP}}{\text{TP} + \text{FP}} \tag{2}$$

$$\text{Recall} = \frac{\text{TP}}{\text{TP} + \text{FN}} \tag{3}$$

$$F1\text{Score} = \frac{2 * \text{Precision} * \text{Recall}}{\text{Precision} + \text{Recall}} \tag{4}$$

$$\text{IoUScore} = \frac{\text{TP}}{\text{TP} + \text{FP} + \text{FN}} \tag{5}$$

Where TP is true positive, FP is false positive, and FN is false negative.

The trained model was evaluated on the test data set using precision, recall, F1-Score and IoU Score. To further investigate the performance of the model, we also calculated the mean absolute difference in frequency of channel

Table 1
Performance of the Attention-UNet Model Over Different Sites

Site	Precision	Recall	F1-Score	IoU Score
Test Area	0.76	0.81	0.79	0.65
Orzano	0.55	0.84	0.66	0.50
Montebelluna	0.90	0.59	0.71	0.56
Montichiari	0.64	0.59	0.61	0.45
Podgorica Airport	0.48	0.66	0.54	0.38

Note. Evaluated metrics are: precision, recall, F1-Score, and IoU Score.

between predictions and ground truths. This value allowed us to check the frequency of pixels assigned to channel in the ground truth and in the predicted tiles, and assess whether the lower values of F1-Score were caused by minor differences in the localization of the palaeochannel boundaries, or in a prediction completely different from the ground truth labels.In the post-processing phase of this work, we applied the trained model to the entire study area (232 km^2). Afterward, we extracted palaeochannel centerlines through skeletonization using the Scikit-Image (version 0.22) library on Python (van der Walt et al., 2014). Centerlines permit to better visualize the quantity of palaeochannels, as well as their direction and braided pattern. Overall, we observed that the direction of the hydrographic traces is from north to south, following the general slope of this sector of the Friulian Plain; therefore, we considered perpendicular west–east transects in order to extract the quantity of channels. Twenty transects were drawn with a spacing of 1 km each, starting from the northern border of the study area. In order to properly extract the number of channels per km we further considered the presence of large vegetated areas and urbanized centers, impeding the identification of traces and proceeded to subtract them from the total length of the transects. Centerlines were used to calculate the number of channels per km over a selection of transects using Python. Channel density–interpreted as the ratio between the area occupied by palaeochannels and the total area–was also extracted from the segmented map.

In order to assess the generalization capability of the trained model, we selected four additional test sites characterized by braided palaeohydrographic traces. In the case of the Orzano site, which is also located in the Friulian Plain, the input data set consists of orthophotos from the same data set as the main study area. As for the other case studies, we selected satellite images from the Google Earth platform (images from Maxar Technologies) with similar HSV (hue, saturation and value) of the original data set, down sampling them to 1 m resolution (12 May 2012 image for Montebelluna, 11 May 2009 image for Montichiari, 18 May 2012 image for Montenegro). The same preprocessing steps as before were used, manually labeling palaeochannels and subdividing input images into 256 × 256 px tiles. Afterward, we evaluated the trained model on the new sites, assessing the same metrics.

To obtain a visual explanation of the identification made by the Attention-UNet algorithm, we decided to implement saliency maps both on the main test data set and on the four additional sites in Python using TensorFlow. Saliency maps provide a way to decipher black-box models represented by CNNs, shedding information on the generalization capability of the trained models and on which features are the most important in the prediction of classes (Szczepankiewicz et al., 2023). We used Gradient-weighted Class Activation Mapping (Grad-CAM) as proposed by Selvaraju et al. (2020), which applies a gradient-based weighting to class activation maps. It uses gradients associated to the class computed on the last layer to produce a heat map that highlights regions of the image that have the greatest impact on network prediction. The choice of this method of visual explanation is based on the results of the comparison of different saliency maps described in Szczepankiewicz et al. (2023). Grad-CAM heat maps were computed on the last concatenation layer of the decoder part of the Attention-Unet, which reflects the regions contributing to the output segmentation by also integrating the importance of the attention gates used in the upsampling part of the UNet.

3. Results

The model took 150 training epochs to converge. On the test data set it reached an F1-Score of 0.79 (Table 1). The histogram of F1-Score highlighted that the majority of the predicted tiles had an F1-Score higher than 0.8, although a tail of very low values was present (Figure 5). We observed that these values correspond to tiles characterized by dense vegetation (mainly woods, but sometimes also crops) or by an obvious overlapped anthropogenic pattern (i.e., built areas or pervasive field division systems), where the model struggled to correctly identify palaeochannels. In general, however, lower F1-Scores were mainly the result of minimum differences in placing the edges of the channels between the predicted and the ground truth labels (Figure 6).

The model showed a considerate ability to learn channel continuity and ignore interfering road segments in the test data set. Although specific infrastructures–mainly the largest ones–remain problematic for the trained model (Figure 6b), the UNet was successfully able to preserve the palaeohydrographic continuity in the final segmented map of the study area. Despite this ability being obtained at the expense of a decrease in all metrics scores in the

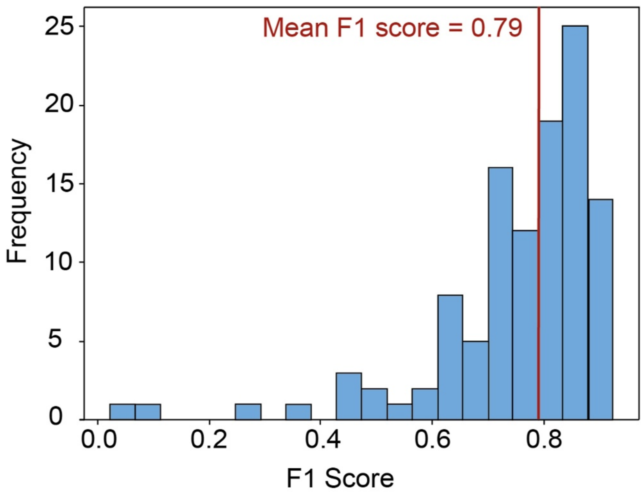

Figure 5. Histogram evaluating F1-Score in the test data set.

test data set–from F1-Score = 0.84 to F1-Score = 0.79–we argue that the usefulness of the model greatly increased as did the geomorphological meaning of the final map.

To assess the generalization capability of the trained model, we selected four additional test sites, at increasing distances from the main study area. The comparison with the training site displays lower values of F1-Score in all the new cases, ranging from 0.71 in the Montebelluna site, to 0.54 in the Podgorica Airport site. The same was also reflected in all the other metrics (Table 1).

Grad-CAM was calculated on the main test data and on the additional sites to visualize which regions of one image contributed the most to the palaeochannel identification. The resulting heat maps highlight that the model correctly assigns a larger importance to the darker palaeochannel traces and much lower to the lighter background areas (Figure 7). Furthermore, the highest values in the heat maps are often found at the edges of the palaeochannels, suggesting that the model relies on the stark chromatic change between channel and bars to identify the presence of the palaeohydrography. Conversely, the impact of intersecting roads, urban structures and vegetated fields is evident in the alternating high and low importance that the algorithm might wrongly assign to some of these regions (see Figures 7b, 7c and 7d).

Deploying the trained Attention-UNet model allowed us to map LGM braided palaeochannels over an area of 232 km^2, corresponding to a significant sector of the Friulian Plain. Centerlines were extracted in order to assess the quantity of palaeochannels and their braided patterns. We found the mean number of channels per km to be 14, varying from a maximum of 18 to a minimum of 10. Compared to the present-day Tagliamento River, the mean number of active channels per cross-section–around 1 km in width–is 4 (Egozi & Ashmore, 2008; Surian & Rinaldi, 2003). However, if historical cartography from the 19th century is considered, the number of active channels of the Tagliamento River in the study area is approximately 10 (Surian et al., 2009).

The binary map segmented by the Attention-UNet model was also used to calculate the density of the palaeochannels, essentially corresponding to the ratio between the area occupied by channels and the size of the kernel–equal to 16 km^2. The choice of the kernel size was mostly a compromise between the widths of the channels, the size of the urban centers, and the spatial resolution of the map. In order to properly compare densities through the site, we subtracted vast urban and forested areas from the original density. We found that, over the study area, the palaeochannel density varies from 69.1% to 44.7% with a mean density of 53.5%, indicating that more than half of the top surface is occupied by palaeohydrographic traces.

4. Discussion

This work successfully trained a deep learning model to segment braided palaeochannels, demonstrating the ability of these type of algorithms to recognize a complex multichannel pattern of palaeohydrography despite the presence of overlaying human infrastructures and agricultural land divisions. In the study area, the pervasive intersection of roads and the different patches of crops represent the main pattern in optical remotely sensed images. Successful segmentation of palaeochannels in their natural continuity, ignoring intersecting urban infrastructures, constitutes the main difficulty when training AI algorithms to identify geomorphological features in a densely cultivated plain. It is likely that this is also the main reason why this methodology has seldomly been attempted in this field of study. Conversely, our findings demonstrate that the recognition of the underlying palaeohydrographic pattern in these settings can be successfully obtained from deep learning.

We found the positive performance of the Attention-UNet model to be in agreement with the geoscience literature using this algorithm. Multiple studies have applied this model to segment landslides using either LiDAR, optical, or SAR data sets (e.g., Fang et al., 2022; Nava et al., 2022; Shi et al., 2023; Zhang, B. et al., 2024) obtaining F1 F1-Scores between 0.61 and 0.87, depending on the type of remotely sensed data. As for palaeochannel detection, despite the current lack of papers focusing on their identification, Zhong et al. (2024) successfully used the algorithm to recognize fluvial landforms in seismic stratigraphic images reporting an F1-Score of 0.85. Our

10.1029/2024JF008051

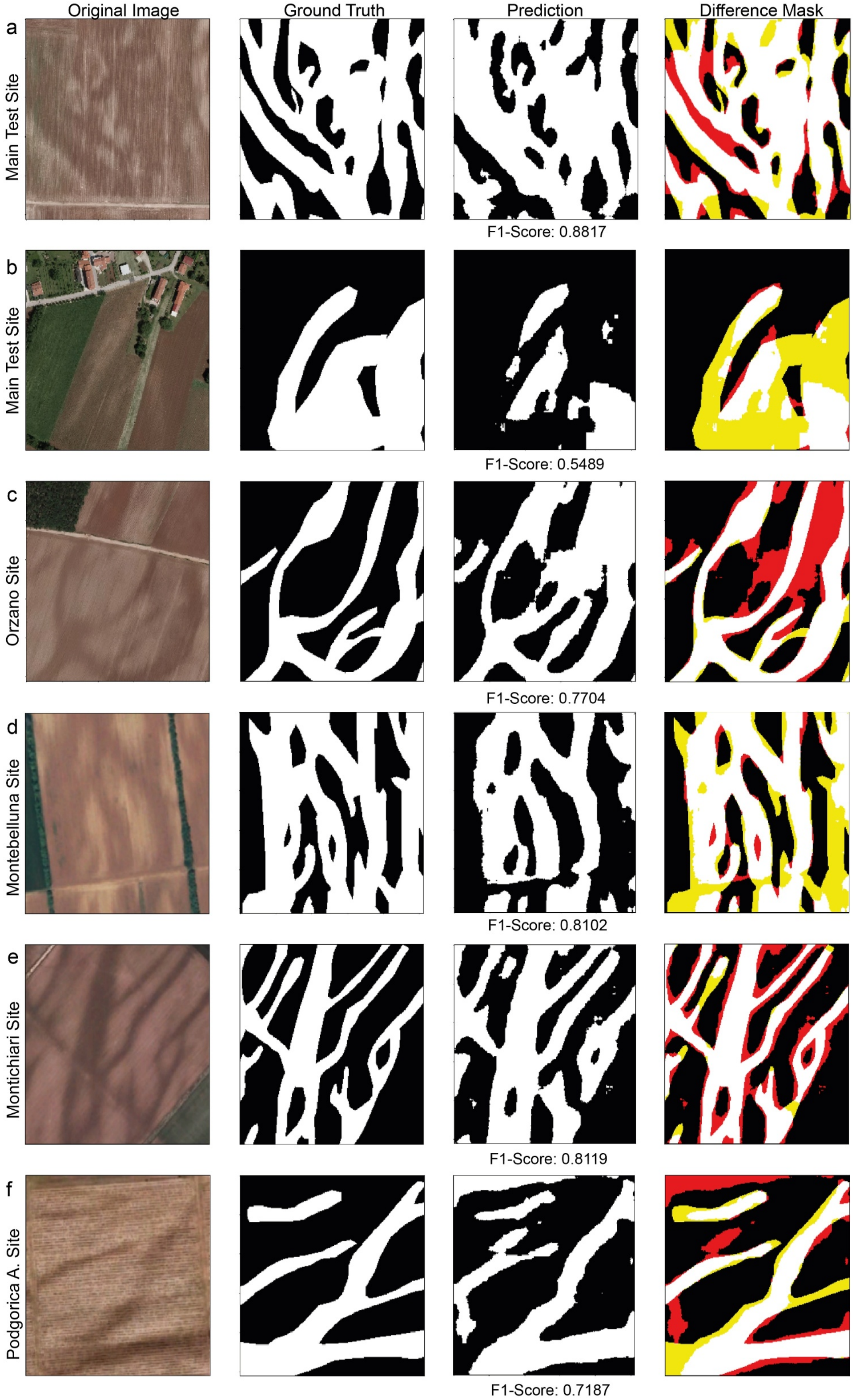

Figure 6. Inputs and output tiles of the Attention-UNet model. The dimension of each tile is 256 × 256 m. In the Difference Mask, the colors are white for true positive, black for true negative, red for false positive, and yellow for false negative. (a, b) Test Area Site; (c) Orzano Site; (d) Montebelluna Site; (e) Montichiari Site; (f) Podgorica Airport Site.

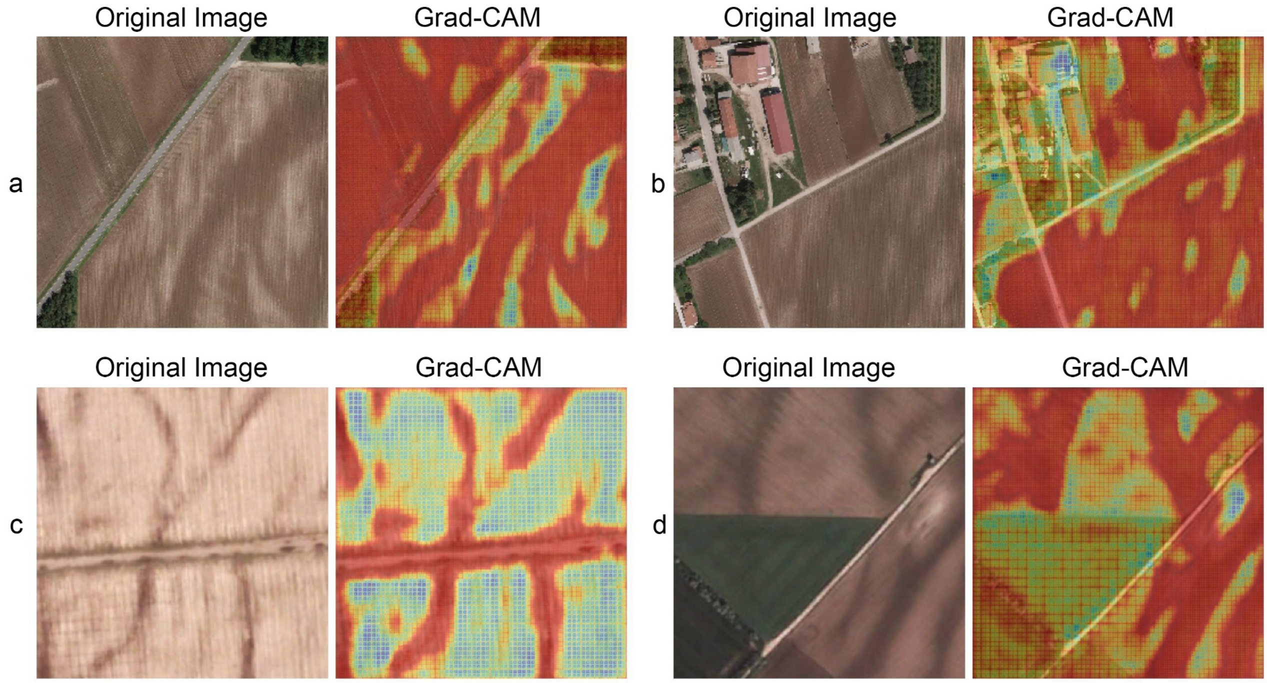

Figure 7. Original images and Grad-CAM heat maps. In blue lowest values, in dark red highest values. (a) Main study area, notice the highest values in correspondence of the palaeochannel edges and the lower value on the road; (b) main study area; (c) Podgorica Airport site; (d) Montichiari site.

findings underline the potential of attention gates in UNet models for identifying and segmenting palaohydrography also in optical remotely sensed images.

Moreover, the model demonstrated to generalize well even outside of the training and testing study area, as highlighted by the identification of braided palaeohydrographic traces formed by different fluvial systems, in different land use settings. The drop in performance observed in the additional testing sites is mainly related to a number of differences characterizing the case studies such as the diverse data set source, the land use, the size of the palaeochannels, and the spectral signature of the traces (Figure 6). More in detail, the data set of orthophotos analyzed in the training area is not available in Montebelluna, Montichiari, and Podgorica , and consequently, high-resolution images from the Google Earth platform were used as input data sets. The variation in acquisition date and location inheritably carries a variance in the RGB spectral signature of the argillic soils overlaying palaeochannels and the gravelly sediment overlaying fluvial bars. In the cases of Montichiari and Podgorica Airport, as well as Orzano–for which we used the original Civil Protection data set–the narrower size of the palaochannels is also a determining factor in the lower performance of the model, which tends to overestimate the width of the channels compared to the ground truth labels. Finally, in the Podgorica Airport site, the farmland is mainly occupied by orchards, whose linear layout adds noise to the palaeohydrographic pattern, constituting the main cause of the lower F1-Score in the case study. Despite all these limitations, the model demonstrated an ability to recognize the presence of braided palaeochannels in the majority of the sites. These findings are particularly important as they suggest that deep learning models trained to identify palaeohydrography in the Friulian Plain could also be implemented on a broader scale, and used to extract information on other alluvial plains characterized by similar optical traces in Italy and elsewhere.

The possibility of rapidly obtaining large, detailed maps of the spatial distribution and morphology of the palaeochannels can strongly assist and improve the geomorphological research. Specifically, manual mapping these multichannel traces is very time consuming, whilst the model trained in this work could allow for a rapid deployment on new sites without requiring for a full-scale manual labeling effort. Nevertheless, it is important to stress out that the ability of the trained algorithm to identify the palaeochannels is highly dependent on the quality of the manual labeling activity in the pre-processing phase. In particular, the ability of the human operator to correctly identify the braided channels and select the boundaries of the geomorphological traces is complicated by the complex multichannel pattern. Therefore, the selection of a training data set characterized by an exceptional

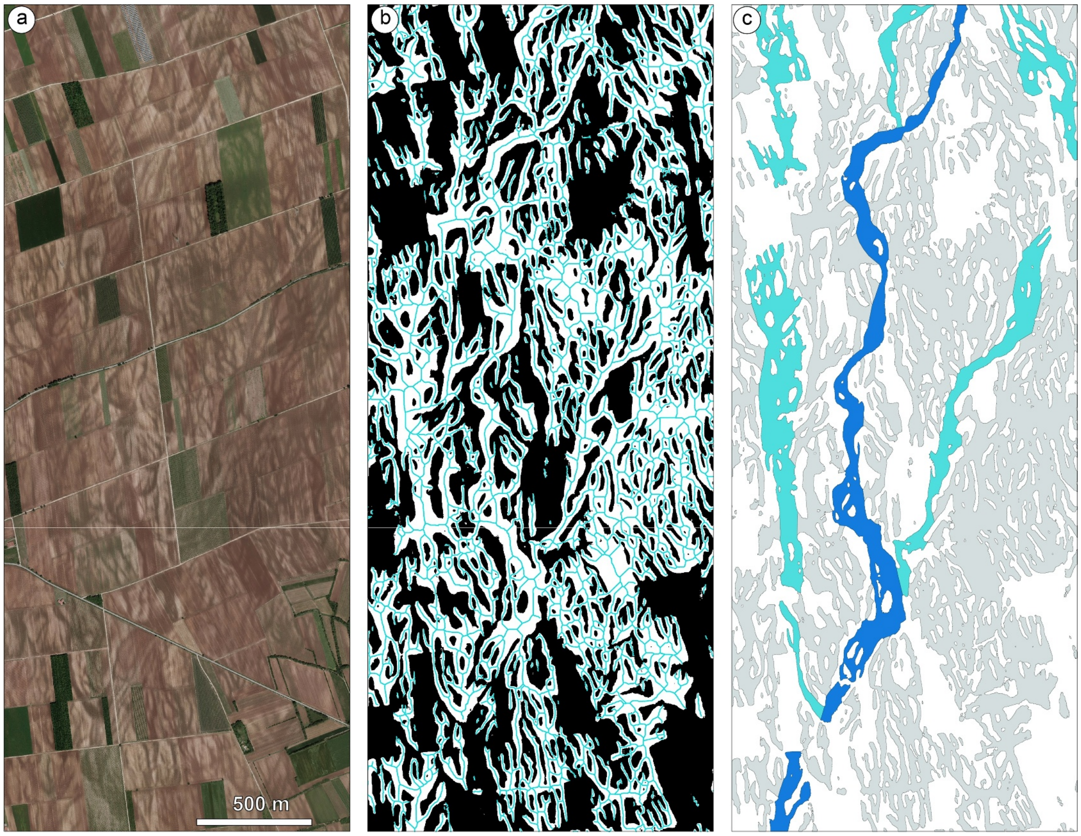

Figure 8. End to end implementation of palaeochannel segmentation. (a) A sub sector of the main study area aerial photo; (b) segmentation and skeletonization of the palaeochannels resulting from the deep learning model workflow, palaeochannels are in white, background in black, skeleton in blue. The large background patches correspond to the vegetated fields in (a); (c) the final interpretation depicting darker shades of blue for evidencing some of the main channel belts.

visibility and clarity of the palaeohydrographic traces was critical to reduce uncertainties through the creation of the labeled data set.

The results of the model also show the effect of the main anthropogenic features hampering the detection of traces. Intersecting roads, urban structures and vegetated fields obstruct the visibility of the underlying palaeochannels, and complicate efforts to map the palaeohydrography in its continuity. Whilst the presence of roads was partly resolved through the creation of a ground truth data set where intersecting pathways were ignored in order to encourage the model to understand channel continuity, the other two elements remain a critical issue. In fact, both urban structures and vegetated fields prevent the identification of the RGB chromatic difference used to identify the palaeochannels (Figure 3), and lead to the creation of blank spots in the resulting map in correspondence to these areas (Figure 8). These spots do not indicate the lack of palaeohydrographic traces, but rather the absence of data from which it would be possible to map their pattern, leading to the inevitable interruption of channel continuity. Notwithstanding, this limit is not restricted to the application of the Attention-UNet model, but also applies to traditional manual mapping, and it is one of the main obstacles in the detection of these traces in a partially urbanized alluvial plain setting such as those identified by this work.

The investigation of the Grad-CAM heat maps was of critical importance to understand how and why the Attention-UNet model was able to identify the braided palaeohydrography. Results allowed us to confirm that the algorithm was based on the identification of the right features, and explain its ability to generalize on the additional test sites (Figure 7). Furthermore, assessing which regions are most important for the identification of the features gave insight into how the model defines the geomorphological traces. Heat maps show that the algorithm relies on the stark chromatic contrast at the edge of palaeochannel traces, as well as on the darker spectral signature of the clay overlaying the channels as a whole. This decisioning is in line with the method used by the user to create the ground truth data set, and the one commonly used in traditional manual mapping of palaeohydrographic evidence. Therefore, we found that the careful selection of a data set where the spectral signature of these geomorphological elements displays a high contrast with the background is the key element for a successful reconstruction of the braided pattern, both in the case of human and deep learning based mapping.

Nevertheless, the resulting palaeohydrographic map highlights that this method can assist in the characterization of the spatial distribution and planar morphology of these traces over hundreds of km^2. Whereas previous works relied on the precise manual mapping of palaeochannels over limited areas and with a rather recent age (e.g., Chandler et al., 2017; Evans & Orton, 2014; Waller et al., 2018), we found that AI models can successfully improve time efficiency and increase the scale of investigation, encouraging the description of complex and often neglected relict features in alluvial plain environments.

Furthermore, these maps of palaeohydrographic traces will provide a plethora of new data related to the abundance, the morphometry, and the directions of the ancient channel belts (Figure 8). These are key data for unlocking the ability to assess the ancient fluvial processes that led to the formation of the alluvial plains in their apical sector, aiming to detect, separate and characterize the main channel belts. In particular, considering the study area in Friuli Venezia Giulia, the new maps generated by deep learning application could support investigations about the imprint of LGM glaciers in the alluvial plain, as well as compare modes and times of activity of the different outwash streams that were fed by different sectors of the same glacier, supplied by the Tagliamento catchment. At present, even if some geomorphological sub-units might be distinguished in the plain dominated by braided traces, according to the orientation and morphometry of the palaeochannels, generally it is not easy to recognize the channels that were really active at the same time and to delimit the boundary of a channel belt. It is worth noting this limit as it is of crucial importance for any geomorphic and hydrographic characteristic that one might want to extract from the palaeohydrographic maps. Thus, channel densities calculation, as well as the estimation of the number of channels per kilometres might be misleading, and should be cautiously compared with present-day braiding indexes. Therefore, in this work we provided these calculations tentatively, mainly to show the potential information supported by these new maps and not to present a quantitative comparison between ancient and present Tagliamento braided channels.

It is also significant to note that the optical traces identified and mapped in this work consist of LGM gravelly sediments that have been later affected by the pedogenesis and strongly impacted by the modern anthropogenic activity. Consequently, an issue arises if palaeochannel widths are considered. In fact, the boundaries of a fluvial trace are mapped according to the limit existing between the dark color of the soil over the palaeochannel and the lighter one on the fluvial bar (Figure 3). Thus, different intensities and timespans of agricultural activities are leading to changes in the palaeochannel widths detected through visible images. In particular, as deeper plowing is progressively eroding a thicker portion of soil, even in the short term, this process exposes wider portions of gravelly fluvioglacial sediments, in turn probably reducing the widths of the fluvial traces and their visibility.

Despite the limitations listed above, we are confident that deep learning algorithms such as the one used in this work could offer new perspectives and possibilities to landscape evolution studies and Quaternary mapping. The successful deployment of our AI model over a study area of 232 km^2 illustrates how studies could overcome the struggles of manually mapping complex features, such as braided patters, and almost instantaneously obtain a geomorphological map of specific landforms. The promising results achieved on different alluvial plains suggest that these models can generalize well on a regional and possibly even global scale. Furthermore, similar architectures could be tuned to identify a broad variety of different geomorphologicals and potentially gearchaeological traces. Examples of some other features that could be recognized are dolines, tidal channels, aeolian dunes, and ancient roads and settlements. Finally, automatically segmented maps of palaeochannels can constitute a valuable base for a complete geomorphological map, for the identification of channel belts and flow directions, and for the differentiation of different fluvial units (Figure 8).

5. Conclusions

In this paper, we trained and tested a deep learning algorithm to identify and map braided palaeochannel traces on alluvial plains using remotely sensed optical data. The Attention-UNet architecture was chosen and trained on 21,874 images of 256 × 256 m of size. On the test data set, we obtained an F1-Score equal to 0.79. Afterward, we deployed the trained model over an area of 232 km^2 located in the Friulian Plain and successfully mapped the traces of braided channels, which cover 53.5% of the entire zone, with an average of 14 channels per km. The model was further tested on four other alluvial plains formed during the late Pleistocene in Friuli Venezia Giulia, Veneto, and Lombard regions in northern Italy, and in the alluvial fan of the Cem River near Podgorica in Montenegro. The results show good generalization potential despite local differences, suggesting that the model could be implemented in other similar settings at a regional scale. Through our findings, we argue that deep learning algorithms can offer great advantages and breakthrough potential to late Quaternary landscape studies focusing on cultivated and partly urbanized settings, and complex landform patterns.

Conflict of Interest

The authors declare no conflicts of interest relevant to this study.

Data Availability Statement

Version 1.3.1 of Albumentation used for performing data augmentation in the pre-processing of the images is based on Buslaev et al. (2020) developed at https://github.com/albumentations-team/albumentations. Version 0.22 of Scikit-Image used to skeletonize the segmented palaeochannels is based on van der Walt et al. (2014) developed at https://scikit-image.org/. The aerial photo data set used for training the model and to implement the trained model on the entire study area is available at https://geodati.gov.it/resource/id/r_friuve:m10603-cc-i10641. The python code, test data sets, model weights and results discussed in this study are preserved at Zenodo via Vanzani et al. (2024). Additional Supporting Information S1 is also available in Zenodo via Vanzani et al. (2024).

Acknowledgments

This research was funded by the University of Padova, project DOR2023139/20, and partly also by the "The Geosciences for Sustainable Development" project (Budget Ministero dell'Università e della Ricerca-Dipartimenti di Eccellenza, 2023–2027C93C23002690001). The authors thank Lorenzo Nava for his suggestions on the Attention-UNet model. Open access publishing facilitated by Universita degli Studi di Padova, as part of the Wiley - CRUI-CARE agreement.

References

Abraham, N., & Khan, N. M. (2018). A Novel Focal Tversky loss function with improved Attention U-Net for lesion segmentation (Version 1). *arXiv*. https://doi.org/10.48550/ARXIV.1810.07842

Berendsen, H. J. A. & Stouthamer, E. (Eds.) (2001)., *Paleogeographic development of the Rhine–Meuse Delta*. Assen:Van Gorcum.

Bertoldi, W., Gurnell, A., Surian, N., Tockner, K., Zanoni, L., Ziliani, L., & Zolezzi, G. (2009). Understanding reference processes: Linkages between river flows, sediment dynamics and vegetated landforms along the Tagliamento River, Italy. *River Research and Applications*, *25*(5), 501–516. https://doi.org/10.1002/rra.1233

Bondesan, A., Busoni, S., Levorato, C., & Meneghel, M. (2015). Geomorphological map of the province of Treviso. Scale 1:50,000. *Crocetta del Montello: Grafiche Antiga*.

Bridge, J. S. (Ed.) (2003). *Rivers and floodplains: Forms, processes, and sedimentary record*. Blackwell Science.

Brown, A. G. (Ed.) (1997). *Alluvial geoarchaeology: Floodplain archaeology and environmental change*. Cambridge University Press.

Buslaev, A., Iglovikov, V. I., Khvedchenya, E., Parinov, A., Druzhinin, M., & Kalinin, A. A. (2020). Albumentations: Fast and flexible image augmentations. Information [Software]. *Git-Hub*, *11*(2), 125. https://doi.org/10.3390/info11020125

Camps-Valls, G., Tuia, D., Zhu, X. X., & Reichstein, M. (Eds.) (2021). *Deep learning for the Earth sciences: A comprehensive approach to remote sensing, climate science, and geosciences* (1st ed.), John Wiley. https://doi.org/10.1002/9781119646181

Carbonneau, P. E., Belletti, B., Micotti, M., Lastoria, B., Casaioli, M., Mariani, S., et al. (2020). UAV-based training for fully fuzzy classification of Sentinel-2 fluvial scenes. *Earth Surface Processes and Landforms*, *45*(13), 3120–3140. https://doi.org/10.1002/esp.4955

Carbonneau, P. E., & Bizzi, S. (2024). Global mapping of river sediment bars. *Earth Surface Processes and Landforms*, *49*(1), 15–23. https://doi.org/10.1002/esp.5739

Carbonneau, P. E., Dugdale, S. J., Breckon, T. P., Dietrich, J. T., Fonstad, M. A., Miyamoto, H., & Woodget, A. S. (2020). Adopting deep learning methods for airborne RGB fluvial scene classification. *Remote Sensing of Environment*, *251*, 112107. https://doi.org/10.1016/j.rse.2020.112107

Cassiani, G., Bellizia, E., Fontana, A., Boaga, J., D'Alpaos, A., & Ghinassi, M. (2020). Geophysical and sedimentological investigations integrate remote-sensing data to depict geometry of fluvial sedimentary bodies: An example from Holocene point-bar deposits of the Venetian plain (Italy). *Remote Sensing*, *12*(16), 2568. https://doi.org/10.3390/rs12162568

Chandler, B. M., Evans, D. J., Chandler, S. J., Ewertowski, M. W., Lovell, H., Roberts, D. H., et al. (2017). The glacial landsystem of Fjallsjökull, Iceland: Spatial and temporal evolution of process-form regimes at an active temperate glacier. *Geomorphology*, *361*, 107192. https://doi.org/10.1016/j.geomorph.2020.107192

Chen, L.-C., Papandreou, G., Kokkinos, I., Murphy, K., & Yuille, A. L. (2018). DeepLab: Semantic image segmentation with deep convolutional nets, Atrous convolution, and fully connected CRFs. *IEEE Transactions on Pattern Analysis and Machine Intelligence*, *40*(4), 834–848. https://doi.org/10.1109/TPAMI.2017.2699184

Cordts, M., Omran, M., Ramos, S., Rehfeld, T., Enzweiler, M., Benenson, R., et al. (2016). The cityscapes dataset for semantic urban scene understanding. In *2016 IEEE Conference on Computer Vision and Pattern Recognition (CVPR)* (pp. 3213–3223). Las Vegas, NV: IEEE. https://doi.org/10.1109/CVPR.2016.350

Cortes, C., Mohri, M., & Rostamizadeh, A. (2012). L2 regularization for learning kernels (version 1). *arXiv*. https://doi.org/10.48550/ARXIV.1205.2653

Egozi, R., & Ashmore, P. (2008). Defining and measuring braiding intensity. *Earth Surface Processes and Landforms*, *33*(14), 2121–2138. https://doi.org/10.1002/esp.1658

Evans, D. J. A., & Orton, C. (2014). Heinabergsjökull and skalafellsjökull, Iceland: Active temperate piedmont lobe and outwash head glacial landsystem. *Journal of Maps*, *11*(3), 415–431. https://doi.org/10.1080/17445647.2014.919617

Fang, C., Fan, X., Zhong, H., Lombardo, L., Tanyas, H., & Wang, X. (2022). A novel historical landslide detection approach based on LiDAR and lightweight attention U-net. *Remote Sensing*, *14*(17), 4357. https://doi.org/10.3390/rs14174357

Fontana, A. (Ed.) (2024). *La Pianura del Friuli Venezia Giulia. Geomorfologia e Geologia del Quaternario*. Udine: Regione Friuli Venezia Giulia.

Fontana, A., Monegato, G., Rossato, S., Poli, M., Furlani, S., & Stefani, C. (2019). *Carta delle unità geologiche della pianura del Friuli Venezia Giulia alla scala 1:150.000 e note illustrative*. Udine: Regione Autonoma Friuli Venezia Giulia—Servizio Geologico.

Fontana, A., Monegato, G., Zavagno, E., Devoto, S., Burla, I., & Cucchi, F. (2014). Evolution of an Alpine fluvioglacial system at the LGM decay: The Cormor megafan (NE Italy). *Geomorphology*, *204*, 136–153. https://doi.org/10.1016/j.geomorph.2013.07.034

Fontana, A., Mozzi, P., & Bondesan, A. (2008). Alluvial megafans in the Venetian-Friulian plain (North-Eastern Italy): Evidence of sedimentary and erosive phases during late Pleistocene and Holocene. *Quaternary International*, *189*(1), 71–90. https://doi.org/10.1016/j.quaint.2007.08.044

Fontana, A., Mozzi, P., & Marchetti, M. (2014). Alluvial fans and megafans along the southern side of the Alps. *Sedimentary Geology*, *301*, 150–171. https://doi.org/10.1016/j.sedgeo.2013.09.003

Gibling, M. (Ed.) (2021). *Rivers from deep time to the modern crisis*. Liverpool: Liverpool University Press.

He, K., Zhang, X., Ren, S., & Sun, J. (2015). Delving deep into rectifiers: Surpassing human-level performance on ImageNet classification. In *2015 IEEE International Conference on Computer Vision (ICCV)* (pp. 1026–1034). IEEE. https://doi.org/10.1109/ICCV.2015.123

He, K., Zhang, X., Ren, S., & Sun, J. (2016). Deep residual learning for image recognition. In *2016 IEEE Conference on Computer Vision and Pattern Recognition (CVPR)* (pp. 770–778). Las Vegas, NV: IEEE. https://doi.org/10.1109/CVPR.2016.90

Huang, F., Zhang, J., Zhou, C., Wang, Y., Huang, J., & Zhu, L. (2020). A deep learning algorithm using a fully connected sparse autoencoder neural network for landslide susceptibility prediction. *Landslides*, *17*(1), 217–229. https://doi.org/10.1007/s10346-019-01274-9

Hughes, P. D., Woodward, J. C., Van Calsteren, P. C., & Thomas, L. E. (2011). The glacial history of the Dinaric Alps, Montenegro. *Quaternary Science Reviews*, *30*(23–24), 3393–3412. https://doi.org/10.1016/j.quascirev.2011.08.016

Jha, K., Doshi, A., Patel, P., & Shah, M. (2019). A comprehensive review on automation in agriculture using artificial intelligence. *Artificial Intelligence in Agriculture*, *2*, 1–12. https://doi.org/10.1016/j.aiia.2019.05.004

Kabir, S., Patidar, S., Xia, X., Liang, Q., Neal, J., & Pender, G. (2020). A deep convolutional neural network model for rapid prediction of fluvial flood inundation. *Journal of Hydrology*, *590*, 125481. https://doi.org/10.1016/j.jhydrol.2020.125481

Kingma, D. P., & Ba, J. (2014). Adam: A method for Stochastic optimization (version 9). *arXiv*. https://doi.org/10.48550/ARXIV.1412.6980

Kiss, T., Sümeghy, B., & Sipos, G. (2014). Late Quaternary paleodrainage reconstruction of the Maros River Alluvial fan. *Geomorphology*, *204*, 49–60. https://doi.org/10.1016/j.geomorph.2013.07.028

Kussul, N., Lavreniuk, M., Skakun, S., & Shelestov, A. (2017). Deep learning classification of land cover and crop types using remote sensing data. *IEEE Geoscience and Remote Sensing Letters*, *14*(5), 778–782. https://doi.org/10.1109/LGRS.2017.2681128

LeCun, Y., Bengio, Y., & Hinton, G. (2015). Deep learning. *Nature*, *521*(7553), 436–444. https://doi.org/10.1038/nature14539

Litjens, G., Kooi, T., Bejnordi, B. E., Setio, A. A. A., Ciompi, F., Ghafoorian, M., et al. (2017). A survey on deep learning in medical image analysis. *Medical Image Analysis*, *42*, 60–88. https://doi.org/10.1016/j.media.2017.07.005

Liu, Z., Mao, H., Wu, C. Y., Feichtenhofer, C., Darrell, T., & Xie, S. (2022). A ConvNet for the 2020s. In *2022 IEEE/CVF Conference on Computer Vision and Pattern Recognition (CVPR)* (pp. 11966–11976). IEEE. https://doi.org/10.1109/CVPR52688.2022.01167

Long, J., Shelhamer, E., & Darrell, T. (2014). Fully convolutional networks for semantic segmentation (version 2). *arXiv*. https://doi.org/10.48550/ARXIV.1411.4038

Ma, L., Liu, Y., Zhang, X., Ye, Y., Yin, G., & Johnson, B. A. (2019). Deep learning in remote sensing applications:A meta-analysis and review. *ISPRS Journal of Photogrammetry and Remote Sensing*, *152*, 166–177. https://doi.org/10.1016/j.isprsjprs.2019.04.015

Mahammad, S., & Islam, A. (2021). Identification of palaeochannels using optical images and radar data: A study of the damodar fan Delta, India. *Arabian Journal of Geosciences*, *14*(17), 1702. https://doi.org/10.1007/s12517-021-07818-5

Milletari, F., Navab, N., & Ahmadi, S. A. (2016). V-Net: Fully convolutional neural networks for volumetric medical image segmentation. In *2016 fourth International Conference on 3D Vision (3DV)* (pp. 565–571). IEEE. https://doi.org/10.1109/3DV.2016.79

Monegato, G., Ravazzi, C., Donegana, M., Pini, R., Calderoni, G., & Wick, L. (2007). Evidence of a two-fold glacial advance during the last glacial maximum in the Tagliamento end moraine system (Eastern Alps). *Quaternary Research*, *68*(2), 284–302. https://doi.org/10.1016/j.yqres.2007.07.002

Nava, L., Bhuyan, K., Meena, S. R., Monserrat, O., & Catani, F. (2022). Rapid mapping of landslides on SAR data by attention U-net. *Remote Sensing*, *14*(6), 1449. https://doi.org/10.3390/rs14061449

Ninfo, A., Fontana, A., Mozzi, P., & Ferrarese, F. (2009). The map of Altinum, ancestor of Venice. *Science*, *325*(5940), 577. https://doi.org/10.1126/science.117420

Oktay, O., Schlemper, J., Folgoc, L. L., Lee, M., Heinrich, M., Misawa, K., et al. (2018). Attention U-Net: Learning where to look for the pancreas. *arXiv*. https://doi.org/10.48550/arXiv.1804.03999

Oya, M. (1995). Geomorphological maps of alluvial plains and their utilization for mitigation of natural hazards: Flooding and soil liquefaction. *Geographical Review of Japan*, *68B*, 218–242.

Prümers, H., Betancourt, C. J., Iriarte, J., Robinson, M., & Schaich, M. (2022). Lidar reveals pre-Hispanic low-density urbanism in the Bolivian Amazon. *Nature*, *606*(7913), 325–328. https://doi.org/10.1038/s41586-022-04780-4

Radusinović, S., & Pajović, M. (2024). Geology of Montenegro. In G. Barovic (Ed.), *Speleology of Montenegro* (pp. 21–50). Springer. https://doi.org/10.1007/978-3-031-49375-1_3

Ronneberger, O., Fischer, P., & Brox, T. (2015). U-Net: Convolutional networks for biomedical image segmentation (version 1). *arXiv*. https://doi.org/10.48550/ARXIV.1505.04597

Selvaraju, R. R., Cogswell, M., Das, A., Vedantam, R., Parikh, D., & Batra, D. (2020). Grad-CAM: Visual explanations from deep networks via gradient-based localization. *IEEE Transactions on Pattern Analysis and Machine Intelligence*, *128*(2), 336–359. https://doi.org/10.1109/TPAMI.2019.2931283

Shi, X., Wu, Y., Guo, Q., Li, N., Lin, Z., Qiu, H., & Pan, B. (2023). Fast mapping of large-scale landslides in sentinel-1 SAR images using SPAUNet. *IEEE Journal of Selected Topics in Applied Earth Observations and Remote Sensing*, *16*, 7992–8006. https://doi.org/10.1109/JSTARS.2023.3310153

Shorten, C., & Khoshgoftaar, T. M. (2019). A survey on image data augmentation for deep learning. *Journal of Big Data*, *6*(1), 60. https://doi.org/10.1186/s40537-019-0197-0

Srivastava, N., Hinton, G., Krizhevsky, A., Sutskever, I., & Salakhutdinov, R. (2014). Dropout: A simple way to prevent neural networks from overfitting. *Journal of Machine Learning Research*, *15*(56), 1929–1958.

Surian, N., & Rinaldi, M. (2003). Morphological response to river engineering and management in alluvial channels in Italy. *Geomorphology*, *50*(4), 307–326. https://doi.org/10.1016/S0169-555X(02)00219-2

Surian, N., Ziliani, L., Comiti, F., Lenzi, M. A., & Mao, L. (2009). Channel adjustments and alteration of sediment fluxes in gravel-bed rivers of north-eastern Italy: Potentials and limitations for channel recovery. *River Research and Applications*, *25*(5), 551–567. https://doi.org/10.1002/rra.1231

Szczepankiewicz, K., Popowicz, A., Charkiewicz, K., Nałęcz-Charkiewicz, K., Szczepankiewicz, M., Lasota, S., et al. (2023). Ground truth based comparison of saliency maps algorithms. *Scientific Reports*, *13*(1), 16887. https://doi.org/10.1038/s41598-023-42946-w

Tockner, K., Ward, J. V., Arscott, D. B., Edwards, P. J., Kollmann, J., Gurnell, A. M., et al. (2003). The Tagliamento River: A model ecosystem of European importance. *Aquatic Sciences*, *65*(3), 239–253. https://doi.org/10.1007/s00027-003-0699-9

Tozzi, P., & Harari, M. (1984). Eraclea Veneta. Immagine di una città Sepolta. *Parma: Compagnia Generale Ripresaaeree*.

Tuia, D., Marcos, D., Schindler, K., & Le Saux, B. (2021). Deep learning-based semantic segmentation in remote sensing. In G. Camps-Valls, D. Tuia, X. X. Zhu, & M. Reichstein (Eds.), *Deep learning for the Earth sciences* (1st ed., pp. 46–66). Wiley. https://doi.org/10.1002/9781119646181.ch5

van der Walt, S., Schönberger, J. L., Nunez-Iglesias, J., Boulogne, F., Warner, J. D., Yager, N., et al. (2014). Scikit-image: Image processing in Python [Software]. *PeerJ*, *2*, e453. https://doi.org/10.7717/peerj.453

Vanzani, F., Carbonneau, P., & Fontana, A. (2024). Attention-UNet model to segment braided palaeochennels from optical images (3.0) [Dataset]. *Zenodo*. https://doi.org/10.5281/zenodo.13762915

Waller, R. I., Evans, D. J. A., & Hiemstra, J. F. (2018). Glacial landsystem development at Skeiðarárjökull. In D. J. A. Evans (Ed.), *Glacial landsystems of southeast Iceland – quaternary applications: Field guide* (pp. 86–101). Quaternary Research Association.

Zanferrari, A., Avigliano, R., Grandesso, P., Monegato, G., Paiero, G., Poli, M. E., & Stefani, C. (2008). *Note illustrative della Carta geologica d'Italia alla scala 1:50.000 – Foglio 065 "Maniago"*. Graphic Linea.

Zanferrari, A., Avigliano, R., Monegato, G., Paiero, G., & Poli, M. E. (2008). *Note illustrative della Carta geologica d'Italia alla scala 1:50.000 – Foglio 066 "Udine*. Graphic Linea.

Zhang, B., Tang, J., Huan, Y., Song, L., Shah, S. Y. A., & Wang, L. (2024). Multi-scale Convolutional Neural Networks (CNNs) for landslide inventory mapping from remote sensing imagery and Landslide Susceptibility Mapping (LSM). *Geomatics, Natural Hazards and Risk*, *15*(1), 2383309. https://doi.org/10.1080/19475705.2024.2383309

Zhang, S., Ma, Y., Chen, F., Liu, J., Chen, F., Lu, S., et al. (2020). A new method for supporting interpretation of paleochannels in a large scale — Detrended Digital Elevation Model Interpretation. *Geomorphology*, *369*, 107374. https://doi.org/10.1016/j.geomorph.2020.107374

Zhong, D., Wang, J., Guo, Y., Liu, Y., Chen, J., & Xu, T. (2024). A Frangi filter aided deep learning approach for palaeochannel recognition. *Geophysical Journal International*, *236*(3), 1526–1544. https://doi.org/10.1093/gji/ggad491

Ziliani, L., & Surian, N. (2012). Evolutionary trajectory of channel morphology and controlling factors in a large gravel-bed river. *Geomorphology*, *173–174*, 104–117. https://doi.org/10.1016/j.geomorph.2012.06.001